

Detection of Bcl-2 family member Bcl-G in mouse tissues using new monoclonal antibodies

M Giam^{1,2}, JD Mintern^{1,2,3}, GJP Rautureau^{1,4}, MG Hinds^{1,2}, A Strasser^{1,2} and P Bouillet^{*1,2}

Bcl-G is an evolutionarily conserved member of the Bcl-2 family of proteins that has been implicated in regulating apoptosis and cancer. We have generated monoclonal antibodies that specifically recognise mouse Bcl-G and have used these reagents to analyse its tissue distribution and subcellular localisation using western blotting, immunohistochemistry and immunofluorescence. We found that Bcl-G predominantly resides in the cytoplasm and is present in a wide range of mouse tissues, including the spleen, thymus, lung, intestine and testis. Immunohistochemical analyses revealed that Bcl-G is expressed highly in mature spermatids in the testis, CD8⁺ conventional dendritic cells (DCs) in hematopoietic tissues and diverse epithelial cell types, including those lining the gastrointestinal and respiratory tracts. The Bcl-G monoclonal antibodies represent new tools for studying this protein, using a variety of techniques, including immunoprecipitation and flow cytometry.

Cell Death and Disease (2012) 3, e378; doi:10.1038/cddis.2012.117; published online 23 August 2012

Subject Category: Immunity

The Bcl-2 family members are the main regulators of the 'intrinsic' (also called 'Bcl-2-regulated', 'mitochondrial' or 'stress') pathway of apoptosis that is activated by diverse stresses, including DNA damage and cytokine deprivation.¹ These proteins share close homology in up to four characteristic regions, termed the BH (Bcl-2 homology) domains, and can be divided into three subgroups: the pro-survival proteins (Bcl-2, Bcl-xL, Bcl-w, Mcl-1 and A1), the pro-apoptotic multi domain proteins (Bax and Bak) and the pro-apoptotic BH3-only proteins (Bad, Bid, Bik, Bim, Bmf, Hrk, Noxa and Puma). Proteins of the Bcl-2 family control the integrity of the mitochondrial outer membrane and consequently the cytosolic release of apoptogenic proteins, such as cytochrome c and Smac/DIABLO, which promote activation of the caspase cascade that leads to cellular demolition.^{1,2} Several Bcl-2 homology domain (BH)-containing proteins that do not readily fit into either of the above mentioned three subgroups have been described, but their involvement in the Bcl-2-regulated apoptotic pathway is often controversial.³

BCL-G, also known as BCL2L14, was first described as a pro-apoptotic member of the Bcl-2 family.⁴ It is evolutionarily conserved with BCL-G orthologues present in many organisms, including zebrafish. The human *BCL-G* gene contains a putative p53-binding site in its first intron and its expression was reported to be upregulated upon p53 overexpression.⁵ Alternative splicing of the human *BCL-G* transcript produces a long (*BCL-G_L*) and a short (*BCL-G_S*) isoform. Although *BCL-G_L*

mRNA was found in a broad range of tissues, including the lung, pancreas, prostate and testis, *BCL-G_S* mRNA was only detected in the testis.⁴ Overexpression of GFP-tagged proteins in HeLa cells revealed that BCL-G_L is localised diffusely throughout the cytoplasm, whereas BCL-G_S showed a punctate pattern.⁴

BCL-G_S only contains a BH3 domain and has therefore been proposed to function as a pro-apoptotic BH3-only protein by interacting with and neutralising the pro-survival protein BCL-X_L. In contrast, BCL-G_L contains both a BH2 and a BH3 domain. Little is known about the function of this protein, as initial overexpression studies did not reveal significant pro-apoptotic activity.⁴ Subsequent studies have suggested that deregulation of BCL-G expression may exert a role in tumour development. The *BCL-G* gene is located within the human chromosome 12p12 tumour suppressor locus, a region for which loss of heterozygosity has been observed in several haematological malignancies as well as solid tumours.^{6,7} Moreover, it was reported that *BCL-G* mRNA levels are abnormally decreased in breast and prostate cancer samples compared with the corresponding normal tissues.⁷⁻⁹ Maternal embryonic leucine-zipper kinase, a protein overexpressed in many breast cancers and cell lines derived from such tumours, has been shown to bind and downregulate BCL-G_L by phosphorylating it.¹⁰ However, it is not clear whether this effect on BCL-G_L is relevant to tumour development.

¹The Walter and Eliza Hall Institute of Medical Research, Molecular Genetics of Cancer Division, Melbourne, Australia and ²Department of Medical Biology, The University of Melbourne, Melbourne, Australia

*Corresponding author: P Bouillet, The Walter and Eliza Hall Institute of Medical Research, Molecular Genetics of Cancer Division, 1G Royal Parade, Parkville, Victoria 3052, Australia. Tel: +61 3 9345 2334; Fax: +61 3 9347 0852; E-mail: bouillet@wehi.edu.au

³Current address: Department of Biochemistry and Molecular Biology, The University of Melbourne, Melbourne, Australia

⁴Current address: Centre de RMN à Très Hauts Champs, UMR 5280 CNRS/Ecole Normale Supérieure de Lyon, University of Lyon, 5 rue de la Doua, 69100 Villeurbanne, France

Keywords: apoptosis; Bcl-G; Bcl-2 family

Abbreviations: BH domain, Bcl-2 Homology domain; FITC, fluorescein isothiocyanate; ELISA, enzyme-linked immunosorbent assay; HA, haemagglutinin; mAb, monoclonal antibody; DAPI, 4',6-diamidino-2-phenylindole; HRP, horseradish peroxidase; DMEM, Dulbecco's modified Eagle medium; FBS, foetal bovine serum

Received 18.6.12; revised 03.7.12; accepted 11.7.12; Edited by G Raschella

The murine *Bcl-G* gene only produces the Bcl-G_L isoform, which contains both a BH2 and a BH3 domain.¹¹ Like its human counterpart, mBcl-G is highly expressed in the mouse testis but its expression could also be readily detected in many other tissues, including the liver, lung, thymus and spleen.¹¹ In hematopoietic tissues, Bcl-G was reported to be covalently conjugated to the 8.5-kDa ubiquitin-like (Ubi-L) moiety of monoclonal nonspecific suppressor factor beta (also known as Fau) and to display increased mRNA expression in response to mitogen activation of D.10 type 2 T-helper cells.¹¹ The function of the Bcl-G Ubi-L adduct is unclear, but it was proposed to bind and inhibit extracellular signal-regulated kinase activation.¹² Whether this represents a physiological function of Bcl-G is presently unclear.

To elucidate the function of Bcl-G, it was necessary to determine in which tissues and cell types it is expressed. We report here the generation of a panel of monoclonal antibodies (mAbs) specific to murine Bcl-G that can be used in a variety of applications, including western blotting, immunoprecipitation and immunohistochemistry. These mAbs will be critical reagents to study this enigmatic Bcl-2 family member.

Results

Generation and characterisation of monoclonal antibodies against mBcl-G. To produce monoclonal antibodies, we immunised Wistar rats with recombinant full-length mouse Bcl-G. Spleen cells were fused with myeloma cells and the resulting hybridomas screened using flow cytometric analysis¹³ of 293T cells transiently overexpressing haemagglutinin (HA)-tagged mBcl-G (Figure 1a). Fluorescein isothiocyanate (FITC)-conjugated goat antibodies against rat IgG were used as the secondary reagent. Incubation of cells with the secondary antibody alone showed no staining and served as a negative control (Figure 1a). Hybridoma clones producing mAbs specific to Bcl-G yielded a profile similar to that obtained when cells were incubated with HA mAb (positive control, Figure 1a). We selected four hybridoma clones, 2E11, 2F7, 4B10 and 10C9, for future experiments (Table 1). The isotypes of these antibodies were determined by enzyme-linked immunosorbent assay (ELISA): IgG2a κ for 2E11, 10C9 and 2F7 and IgG1 κ for 4B10 (Table 1). Each mAb was purified using protein G affinity columns to be used in various applications.

We further characterised our mAbs by mapping the epitopes that they recognise within the Bcl-G protein. For this, we constructed a panel of 10 deletion mutants of mBcl-G (M1–M10, Figure 2). Each of these mutants lacked a 34-amino-acid-long region (except for M10, which only lacked the 23 C-terminal amino acids). These Bcl-G mutants were transiently overexpressed in 293T cells and protein lysates analysed by western blotting. Detection of these HA-tagged Bcl-G mutants with HA-specific monoclonal antibodies served as a positive control (Figures 2A–C). We found that mAb 2F7 could not detect mutant M7 (Bcl-G Δ 204–237), whereas mAb 4B10 could not detect mutant M10 (Bcl-G Δ 306–328) and mAb 2E11 failed to detect mutant M4 (Bcl-G Δ 102–135; Figure 2A). As mAb 2E11 was the most sensitive of our antibodies, the epitope that it recognises within Bcl-G was further narrowed down using five additional deletion mutants

covering the M4 region (amino acids 102–135). This revealed that mAb 2E11 recognises an epitope localised between amino-acid positions 123 and 135 of mBcl-G (Figure 2B). Intracellular staining of Bcl-G within the transiently transfected 293T cells could also be used to determine the epitope region, as shown for mAb clone 10C9, which, similar to mAb 4B10, binds to a region between the C terminal residues 306–328 of mBcl-G (Figures 2C and D).

Specific detection of endogenous mouse Bcl-G by western blotting and immunoprecipitation. We next used protein lysates from testes to test the ability of our monoclonal antibodies to detect endogenous mBcl-G by western blotting. Lysates from *Bcl-G*^{-/-} testes (Giam *et al.*, accompanying manuscript) were used as negative controls. Three of the four mAbs, 2E11, 2F7 and 4B10, detected an ~38-kDa doublet band in the wild-type testis but not in the *Bcl-G*^{-/-} testis (Figure 3a). No other bands were detected on the western blots, suggesting that these antibodies are highly specific for mBcl-G. In addition, these results confirm that Bcl-G_S does not exist in the mouse. Despite its ability to detect recombinant mBcl-G in 293T cells, mAb 10C9 did not detect endogenous mBcl-G in this experiment (data not shown). Detection of mBcl-G as a doublet probably reveals an as yet uncharacterised post-translational modification of the mBcl-G protein.

We next tested the suitability of our mAbs to immunoprecipitate endogenous Bcl-G from protein lysates of mouse testes. The mAbs 2E11 and 10C9 were both capable of specifically immunoprecipitating endogenous mBcl-G from lysates of WT testes (Figure 3b). In contrast, mAb clones 2F7 and 4B10 did not immunoprecipitate Bcl-G under these experimental conditions (Figure 3b). It therefore appears likely that the epitopes recognised by mAbs 2B7 and 4B10 are hidden when the protein is in its native conformation. We have recently confirmed the ability of the 2E11 and 10C9 mAbs to immunoprecipitate endogenous Bcl-G and associated protein complexes by using lysates from WT intestinal epithelial cells in an experiment designed to identify novel Bcl-G-binding partners (Giam *et al.*, accompanying manuscript).

To determine whether our mAbs could recognise the human BCL-G protein, we tested them on lysates from several human cell lines, including 293T (embryonic kidney cells), HeLa (cervical cancer cells), MDA-231 (breast cancer cells), LNCaP and PC3 (prostate cancer cells). However, no reactivity against hBCL-G protein was detected in western blotting using our mAbs, even though database searches predicted detectable expression of hBCL-G in these cell lines (data not shown). It therefore appears likely that the epitopes recognised by our mAbs are not well conserved between mouse and human Bcl-G.

Immunohistochemical analysis of Bcl-G expression in mouse tissues. Western blotting with clone 2E11 demonstrated that Bcl-G protein is present in a wide variety of organs with especially high levels in the gastrointestinal (GI) tract and testes (Giam *et al.*, accompanying manuscript). We therefore examined the suitability of this particular mAb for immunohistochemical applications, as this would be useful to identify the specific cell types that express Bcl-G in various

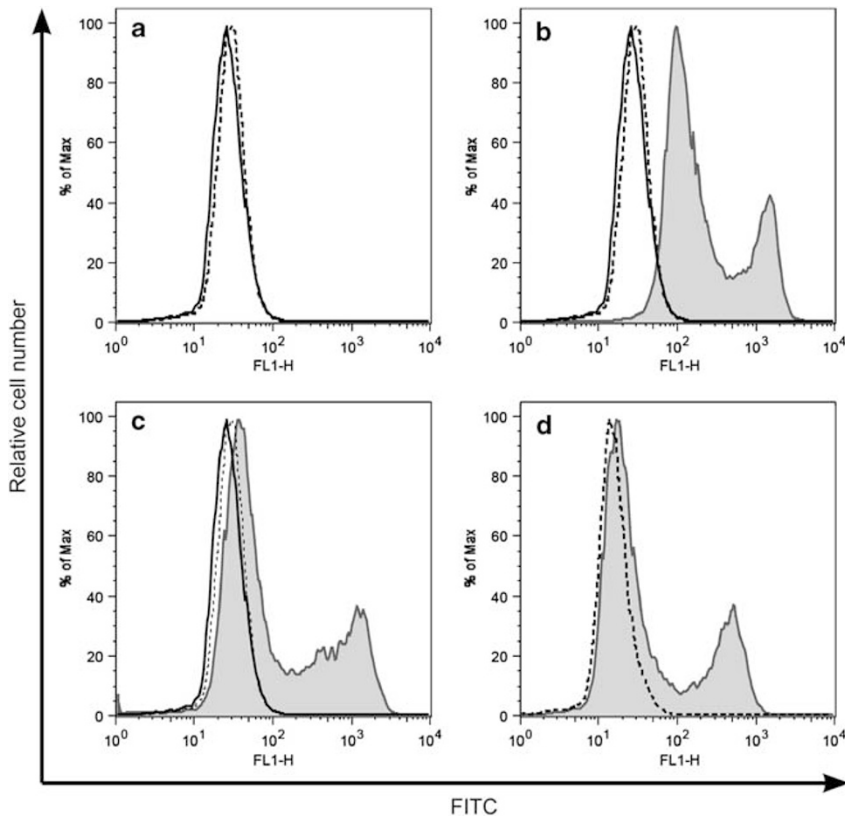


Figure 1 Screening of hybridoma clones for Bcl-G-specific monoclonal antibodies. Hybridoma supernatants were screened for antibodies that detect HA-tagged Bcl-G overexpressed by 293T cells using intracellular immunofluorescent staining and FACS analysis. FITC-conjugated goat anti-rat Ig secondary antibodies (dotted line in **a–c**) were used as the secondary reagent after a first incubation with hybridoma culture supernatant (solid line in **a–c**), sera from immunised rats (**b**) or supernatant from hybridoma clone 2E11 (**c**). Antibodies against HA (dotted line represents FITC-conjugated anti-mouse secondary antibody only, used as a negative control) were used as a positive control (**d**)

Table 1 Summary of the characteristics of the anti-Bcl-G monoclonal antibodies

Antibody clone	Isotype	Epitope	Applications	Species
2E11	IgG2a	102–135	WB, FCM, IP, IF, IH	Mouse
2F7	IgG2a	204–237	WB, FCM	Mouse
4B10	IgG1	306–328	WB, FCM	Mouse
10C9	IgG2a	306–328	IP	Mouse

Abbreviations: FCM, flow cytometry; IF, immunofluorescence; IH, immunohistochemistry; IP, immunoprecipitation; mAb, monoclonal antibody; WB, western blotting. Anti-Bcl-G mAb clones 2E11, 2F7, 4B10 and 10C9 were tested for their ability to detect mouse Bcl-G by WB, FCM, IP, IF, IH. The epitope region refers to the amino-acid position in the mouse Bcl-G reference sequence UniProt Q9CPT0.

organs (Figures 4 and 5). Once again, tissue sections from *Bcl-G*^{-/-} mice provided ideal negative controls. In the testes, intense Bcl-G immunostaining was observed in the late stage spermatids of the germinal epithelium, whereas no staining was seen in the interstitial Leydig cells nor in cells undergoing earlier stages of spermatogenesis (Figure 4a). Bcl-G appears to be downregulated in the last stages of spermiogenesis (maturation of spermatids into mature, motile spermatozoa) as no staining could be seen in the mature sperm in the epididymal tubules (Figure 4a).

In contrast, pronounced staining was observed in the ciliated columnar epithelial cells lining the epididymal ducts (Figure 4a). High-intensity Bcl-G staining was also detected in the epithelial cells lining the secretory alveoli of the prostate, but no staining was seen in the fibromuscular stroma surrounding the glands (Figure 4a).

Bcl-G expression was prominent in the many cells of epithelial origin. Bcl-G staining was observed in the epithelial cells lining the entire GI tract, including those in the small intestine and colon (Figure 4b). In contrast, there was little or no Bcl-G immunoreactivity in the serosa, submucosa and smooth muscle layers within these organs. In addition, certain hematopoietic cells within the Peyer's patches also showed intense Bcl-G staining (data not shown). These were most likely to be the DCs (Giam *et al.*, accompanying manuscript). In the exocrine pancreas, moderate Bcl-G expression was seen in the acinar cells, whereas no Bcl-G staining was detected in the endocrine cells of the islets of Langerhans (Figure 4b). Within the respiratory tract, significant Bcl-G immunoreactivity was observed in the ciliated epithelial cells lining the trachea, which extended through the bronchi of the lungs (Figure 4c). Bcl-G expression in the alveoli seemed to be limited to the type II pneumocytes (Figure 4c), a cell type that secretes surfactants to decrease surface tension within the lung.¹⁴

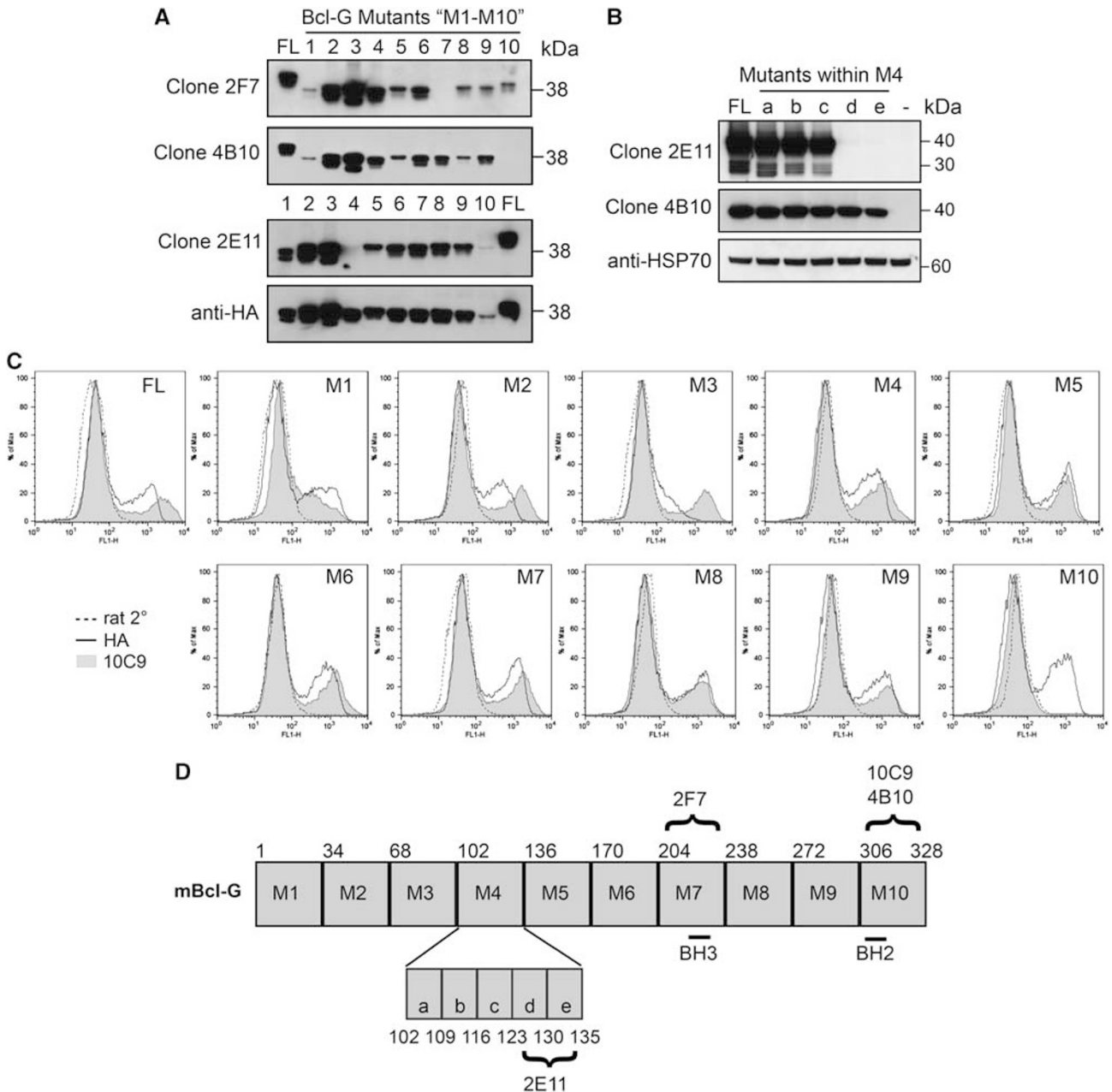


Figure 2 Bcl-G-specific mAbs bind to different regions on mouse Bcl-G. **(A)** A panel of ten truncated Bcl-G deletion mutants (M1–M10) was generated and these proteins overexpressed in 293T cells. The region on Bcl-G recognised by each mAb was determined by testing its ability to detect each Bcl-G truncation mutant in western blotting. Probing with HA-specific antibodies served as a loading control. 'FL' indicates full-length Bcl-G. **(B)** The epitope region recognised by mAb 2E11 was further narrowed using five mutants (a–e) within M4 (amino acids 102–135). '–' indicates extracts from cells transfected with empty vector. **(C)** Intracellular FACS staining of transiently transfected 293T cells was used to map the epitope of mAb 10C9. Cells stained with HA antibody (solid line) or FITC-conjugated anti-rat secondary antibodies (dotted line) were used as positive and negative controls, respectively. **(D)** Schematic diagram of Bcl-G and the epitope regions recognised by each mAb

Specific expression of Bcl-G by epithelial cells was also detected in the bladder, uterus and the stratified squamous epithelia of the tongue (Figure 4d). Strong Bcl-G expression was also observed in the more specialised acinar epithelial cells within exocrine tissues, such as the salivary and lacrimal glands (Figure 4d). Other examples of secretory cells that were found to express Bcl-G include the Paneth and goblet cells found in the intestine.

Consistent with the results obtained by western blotting (Giam *et al.*, accompanying manuscript), no Bcl-G staining

was detected in the liver, brain or kidneys. This stands in contrast to previously published investigations of *Bcl-G* mRNA and Bcl-G protein expression, although the latter used antibodies for western blotting that reveal a band of incorrect size for mBcl-G.¹¹ Finally, no staining in the other tissues examined, including the ovaries, bone, skeletal muscle and heart was observed. Collectively, these results demonstrate that Bcl-G protein is expressed at readily detectable levels in diverse cell types, particularly those of epithelial origin and spermatids.

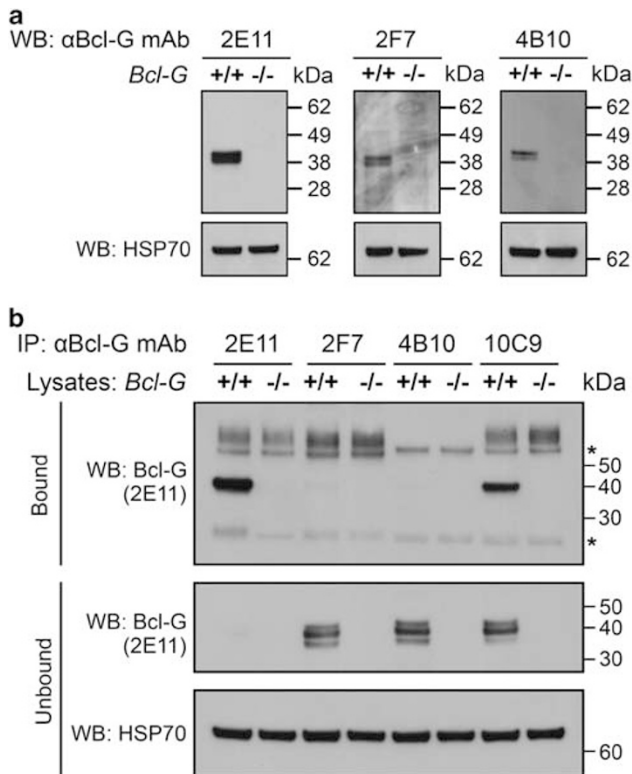


Figure 3 Detection of endogenous Bcl-G by western blotting and immunoprecipitation using Bcl-G-specific monoclonal antibodies. (a) Western blotting using the Bcl-G-specific mAbs 2E11, 2F7 and 4B10 showed that they are capable of specifically detecting endogenous mBcl-G in protein lysates from WT mouse testes. Extracts from *Bcl-G*^{-/-} testes were used as a negative control. Reprobing the membranes for HSP70 served as loading controls. (b) Bcl-G from WT mouse testis lysate was immunoprecipitated using each of the four mAbs and detected in western blots by probing with 2E11. *Bcl-G*^{-/-} testis lysates were used as a negative control. The mAbs 2E11 and 10C9 specifically pulled down endogenous mouse Bcl-G while clones 2F7 and 4B10 did not. Probing for Bcl-G and HSP70 in the flowthrough (unbound) served as loading controls. Asterisks indicate the Ig heavy and light chains

Detection of Bcl-G subcellular localisation using immunofluorescence. We next examined the suitability of our Bcl-G-specific mAb for immunofluorescence staining. To determine the subcellular localisation of Bcl-G, we first used 293T cells transiently transfected with an expression construct encoding full-length mouse Bcl-G. Bcl-G was detected with mAb 2E11 using Alexa488-labelled goat anti-rat Ig antibodies (Molecular Probes, Eugene, OR, USA) as the secondary reagent (Figure 5a). The mitochondria and nuclei of the cells were labelled with Mitotracker Red (Molecular Probes) and 4',6-diamidino-2-phenylindole (DAPI), respectively (Figure 5a). Overexpressed Bcl-G was present throughout the cytoplasm, consistent with with a previous analysis of the subcellular localisation of overexpressed GFP-tagged hBCL-G_L in HeLa cells.⁴

We next used our mAbs to determine the subcellular location of endogenous Bcl-G in the CD8⁺ DCs (Figure 5b), as this was a cell type that exhibited high Bcl-G expression (Giam *et al.*, accompanying manuscript). As was observed with the Bcl-G overexpressed in 293T cells, there was diffuse immunostaining for endogenous Bcl-G in the CD8⁺ DCs, which appeared to be present everywhere in the cytoplasm,

although this staining seemed slightly granular (Figure 5b). As a control for the specificity of this mAb, we could show that no staining was observed in DCs purified from *Bcl-G*^{-/-} mice (data not shown).

We further confirmed the suitability of mAb 2E11 for detecting endogenous Bcl-G by immunofluorescence by staining sections from lymph node (Figure 5c) and testes (Figure 5d). A pattern consistent with DC expression was observed in the lymph node, whereas expression in the mature spermatids was observed in the testis. This application will be very useful to determine co-expression of Bcl-G with other proteins in future studies. We have shown, for example, that Bcl-G is not expressed in the medullary thymic epithelial cells (mTECs) using co-staining with mTEC-specific marker keratin-5 (Giam *et al.*, accompanying manuscript). These results demonstrate that our mAbs to mBcl-G are suitable for immunofluorescent staining to determine sub-cellular localisation in diverse cell types.

Analysis of cells expressing Bcl-G using intracellular staining and FACS. We recently demonstrated by western blotting and immunohistochemistry that conventional DCs within the hematopoietic organs express significant levels of Bcl-G protein, and that the CD8⁺ subset expressed higher levels than the CD8⁻ DC subset (Giam *et al.*, accompanying manuscript). We therefore used DC subsets to test the suitability of our mAbs for flow cytometry. This was done by first staining WT DC-enriched splenocytes with antibodies to the cell surface markers CD11c and CD8 followed by anti-Bcl-G intracellular staining using our mAbs (Figure 6). Although the entire CD11c⁺ population contained significant levels of Bcl-G, the increased Bcl-G content in the CD11c⁺ CD8⁺ subpopulation was clearly evident by the greater shift of the fluorescence histograms, particularly with clone 2E11 (Figure 6). These results indicate our Bcl-G mAbs can be used in intracellular staining and multiparameter flow cytometric analysis, facilitating further studies for the detection and characterisation of Bcl-G-expressing cells in single cell suspensions.

Discussion

Bcl-G was first discovered as a BH-domain-containing protein with pro-apoptotic activity.⁴ However, little progress has been made since then in the elucidation of its physiological function and mechanism of action. To investigate the function of Bcl-G *in vivo*, we needed high-quality antibodies to be able to determine the nature of the cells that normally express this protein. As commercial antibodies available at the commencement of this study detected a 22-kDa band by western blotting, and no Bcl-G isoform was expected to possess that molecular weight, we decided to generate monoclonal antibodies to recombinant mouse Bcl-G. We also produced gene-targeted mice in which the *Bcl-G* gene had been inactivated (described in an accompanying paper, Giam *et al.*), and tissues from these Bcl-G-deficient mice were used in this study to verify the specificity of our antibodies. We report here that we have successfully generated four Bcl-G-specific rat monoclonal antibodies using recombinant full-length mBcl-G as the immunogen. We have determined the Ig

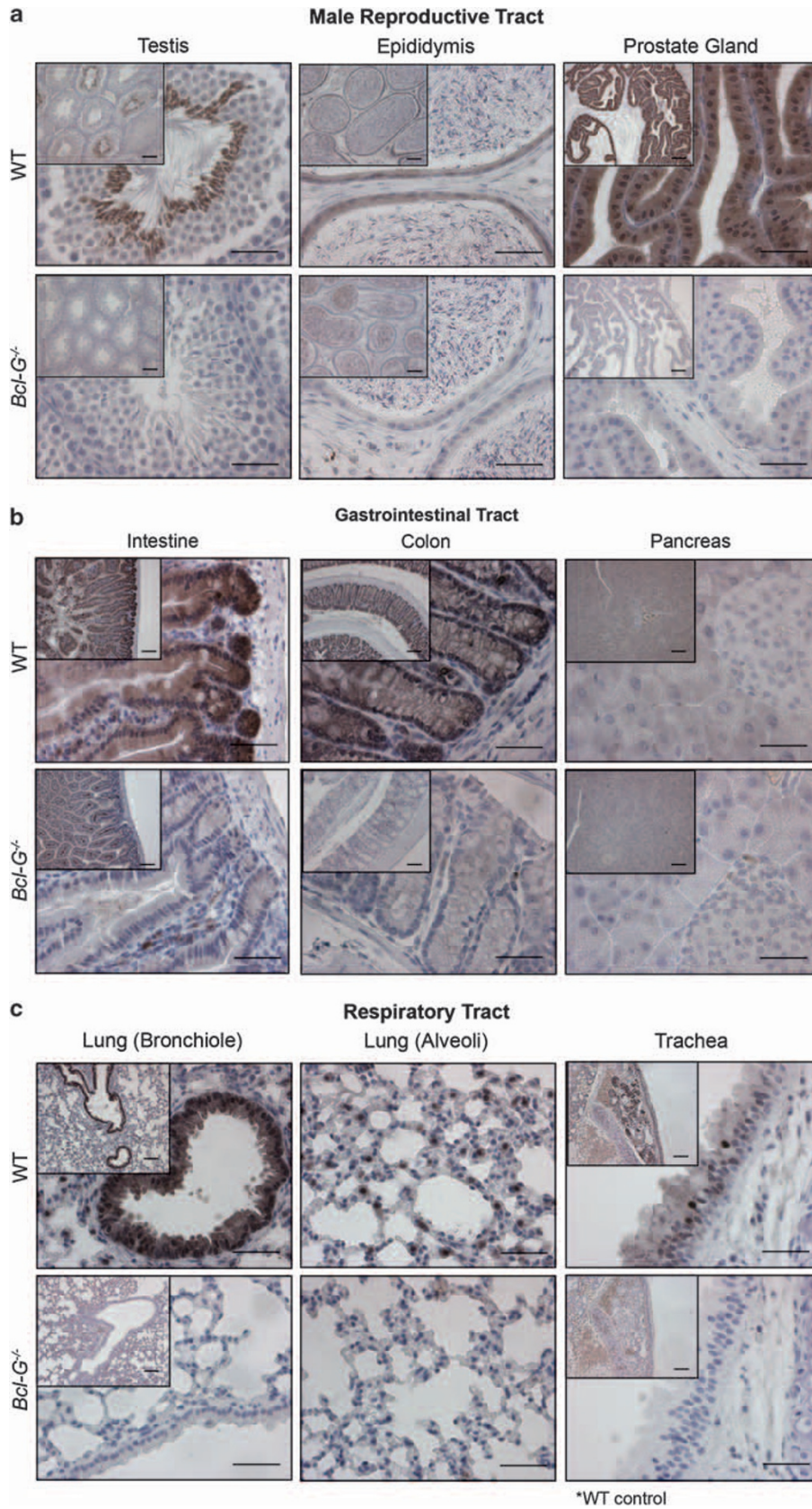


Figure 4 Continued.

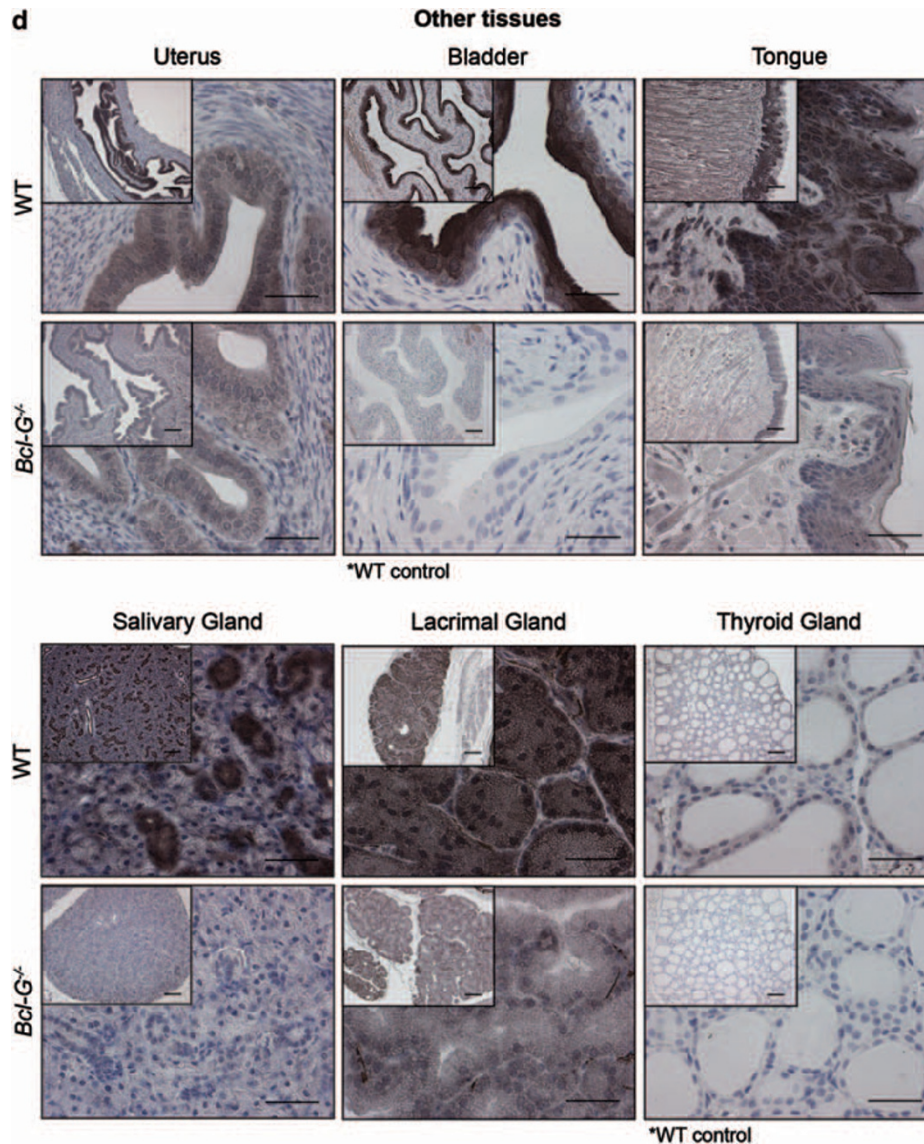


Figure 4 Cell type-specific expression of Bcl-G revealed by immunohistochemical staining. The Bcl-G-specific mAb 2E11 was used for immunohistochemical staining of tissue sections from the (a) male reproductive tract, (b) GI tract, (c) respiratory tract and (d) other organs of WT and *Bcl-G*^{-/-} (negative control) mice. Biotinylated goat anti-rat IgG antibodies were used as the secondary reagent followed by peroxidase conjugation and detection with the DAB reagent (Vector Laboratories). Tissue sections were counterstained with hematoxylin. Representative photomicrographs are shown at $\times 100$ (bar represents $100 \mu\text{m}$) and $\times 400$ magnification (bar represents $40 \mu\text{m}$). The asterisks indicate cases where tissues from *Bcl-G*^{-/-} mice were unavailable and WT tissues stained only with secondary antibodies were used instead as negative controls

isotypes and the epitopes recognised by each of these antibodies and tested their suitability for commonly used experimental applications, including western blotting, immunoprecipitation, immunohistochemistry, immunofluorescence and FACS.

Equipped with these sensitive and specific tools, and using a variety of techniques, we have been able to determine the pattern of expression of Bcl-G down to the level of single cells. This knowledge has guided our analysis of Bcl-G-deficient mice and has also allowed us to investigate biochemical properties of this protein. Only one isoform of Bcl-G is expressed in the mouse, whereas the existence of a non-conserved alternative splice site allows the expression of two different isoforms, hBCL-G_L and hBCL-G_S, in humans.

mBcl-G is similar to the longer human isoform, hBCL-G_L. Interestingly, hBCL-G_L was shown to be poorly pro-apoptotic, if at all.⁴ This has prompted us to design an experiment to identify new binding partners of mBcl-G. As we showed that the intestinal epithelium expresses high levels of mBcl-G, we chose this tissue to produce protein lysates from which mBcl-G was immunoprecipitated using mAbs 2E11 and 10C9. The results, described in an accompanying paper, identified proteins of the transport particle protein complex (TRAPP) as potential partners of Bcl-G, indicating that Bcl-G may be involved in protein trafficking. Importantly, no Bcl-2 family members were identified using this co-immunoprecipitation approach; supporting the notion that mBcl-G may not be involved in the Bcl-2-regulated apoptotic pathway.

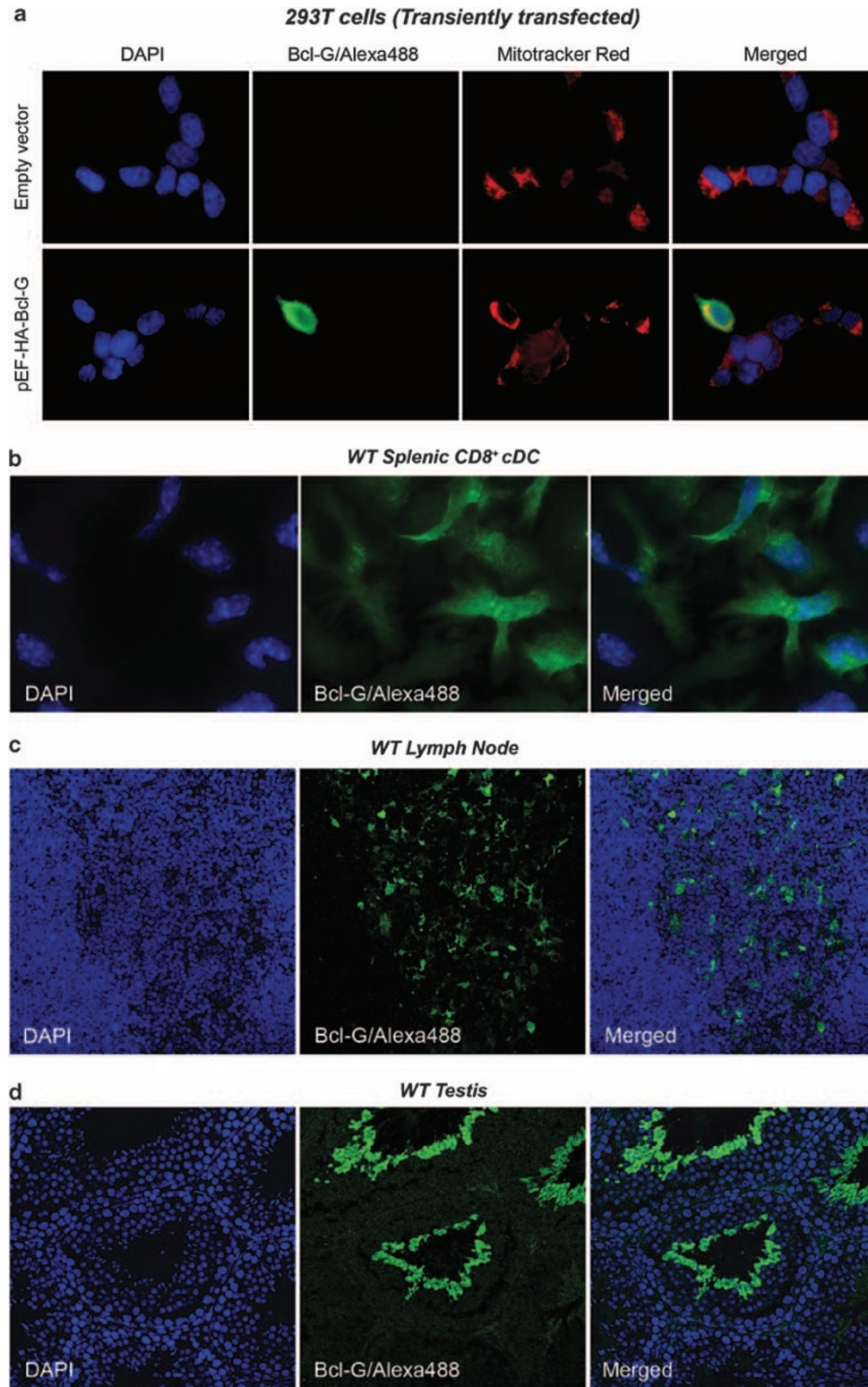


Figure 5 Detection of Bcl-G subcellular localisation using immunofluorescence staining. The Bcl-G-specific mAb clone 2E11 was used in immunofluorescence staining to determine the subcellular localisation of Bcl-G in (a) 293T cells transiently overexpressing HA-tagged Bcl-G or empty vector, (b) FACS-purified splenic CD8⁺ conventional DCs, (c) paraffin-embedded lymph node and (d) testis sections from WT mice. For b–d, *Bcl-G*^{-/-} DCs and control tissue sections that showed no staining (negative controls) are not shown. Bcl-G immunostaining was detected using Alexa488-conjugated goat anti-rat IgG antibodies (Molecular Probes). DAPI and Mitotracker Red (for a) were used to stain the nuclei and mitochondria, respectively

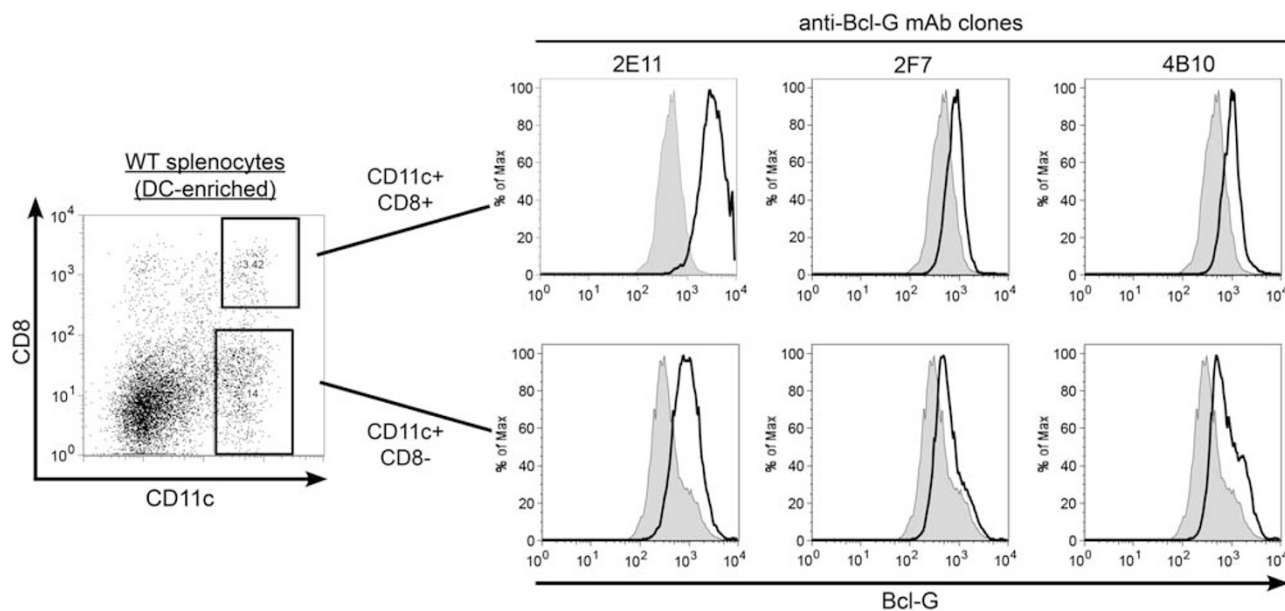


Figure 6 Intracellular staining and FACS analysis using Bcl-G-specific mAbs reveals higher Bcl-G expression in CD8⁺ splenic cDCs compared with other DC subsets. To determine the levels of Bcl-G expression in the CD8⁺ and CD8⁻ DC subsets, DC-enriched splenocyte cell suspensions were surface stained with CD11c-FITC and CD8-APC monoclonal antibodies followed by intracellular staining with biotinylated Bcl-G-specific mAbs and incubation with PE-streptavidin (solid line). Cells stained with PE-streptavidin alone were used as negative controls (tinted grey). Samples were analysed using a flow cytometer and representative FACS plots are shown

Although *Bcl-G* transcripts were previously detected by RT-PCR in the mouse brain, liver and heart tissue,¹¹ we did not detect the protein in these tissues by either western blotting or immunohistochemical analyses. This suggests that post-transcriptional or post-translational mechanisms may have critical roles in regulating the levels of Bcl-G protein expression.

In conclusion, we report here the generation and characterisation of highly specific mAbs for mBcl-G that are useful in an array of experimental applications, including western blotting, immunohistochemistry and flow cytometry. With these antibodies we were able to show that mBcl-G is localised in the cytoplasm and predominantly expressed in a wide range of epithelial cells and in spermatids. These valuable tools and information will facilitate further studies of this novel and unique Bcl-2 family member.

Materials and Methods

Mice. *Bcl-G*^{-/-} mice were generated on a C57BL/6 genetic background as described (Giam *et al.*, accompanying manuscript). C57BL/6 WT mice were obtained from WEHI Bioservices (Kew, Victoria, Australia). All animal procedures were reviewed and approved by the WEHI's Animal Ethics Committee.

Plasmid construction and mutagenesis. The full-length mBcl-G open-reading frame (ORF) was amplified from mouse testis cDNA using the primers (forward: 5'-CGGGATCTGCAGCACCAGTGTGTATGAC and reverse: 5'-CGTCTAGACTCAGTCTACTTCTCATGTGAGAT). The mBcl-G ORF and the mBcl-G mutants were generated using site-directed mutagenesis and subcloned into expression vectors pET-15b (Novagen, Madison, WI, USA) or pEF-HA PGK Hygro (N-terminal HA-epitope tag¹⁵) for bacterial or mammalian cell expression, respectively.

Protein expression and purification. 6His-Bcl-G was expressed at 30 °C in *Escherichia coli* BL21 (DE3) cells following IPTG induction for 3 h. The bacterial cells were resuspended in lysis buffer (50 mM NaH₂PO₄, 300 mM NaCl,

10 mM imidazole, 5 mM β-mercaptoethanol, pH 8) supplemented with complete EDTA-free Protease Inhibitor Cocktail tablets (Roche, NSW, Australia). Soluble protein was extracted by addition of lysozyme (0.2 mg/ml) followed by sonication and centrifugation. His-tagged Bcl-G protein was purified under native conditions using Ni-NTA beads (Qiagen, Chatsworth, CA, USA) according to the manufacturer's instructions. Briefly, the Ni-NTA slurry was added to the bacterial extract, followed by incubation overnight at 4 °C with agitation. The beads were then washed twice with wash buffer (50 mM NaH₂PO₄, 300 mM NaCl, 20 mM imidazole, pH8) and the recombinant protein retrieved with elution buffer (50 mM NaH₂PO₄, 300 mM NaCl, 250 mM imidazole, pH8). The purified recombinant protein was then concentrated using centrifugal filter units (10000 MWCO, Millipore, Bedford, MA, USA) and used for immunisation.

Immunisation. Wistar rats were immunised by injection of 100 μg of purified His-tagged mBcl-G protein. The protein was dissolved in complete Freund's adjuvant (Difco Laboratories, Detroit, MI, USA) and injected subcutaneously. After 3 and 6 weeks, boosts of immunogen resuspended in incomplete Freund's adjuvant were injected subcutaneously. A final boost was given 4 weeks later, followed 3 days later by spleen cell fusion. Rat spleen cells were fused to Sp2/0 mouse myeloma cells using a standard protocol that uses polyethylene glycol-150. Post-fusion, cells were selected in HAT medium (hypoxanthine, aminopterin and thymidine). Fresh medium was added on day 7 post fusion and culture supernatants were harvested for analysis on day 9–11, depending on the rate of hybridoma colony growth. Single-cell cloning was then performed twice to establish stable antibody-producing hybridoma clones.

Screening hybridoma supernatants. Indirect ELISA was used to screen hybridoma supernatants for the presence of mBcl-G-specific antibodies. Ninety-six-well plates were coated with His-tagged mBcl-G protein in carbonate bicarbonate buffer pH 9.6 at 4 °C overnight. Nonspecific antibody-binding sites on the plates were then blocked with 5% (w/v) skim milk in PBS for 1 h at 37 °C. Serially diluted serum samples from immunised rats or supernatants from hybridoma clones were then added in duplicates and incubated for 1 h at 37 °C. Bound antibodies were detected by using rabbit antibodies against rat IgG that had been conjugated with horseradish peroxidase (HRP) and bound complexes were revealed by staining with tetramethyl-benzidine (KBL, Gaithersburg, MD, USA) and H₂O₂. Colorimetric signals were measured at 450 nm. Individual hybridoma clones were cultured in hybridoma serum-free medium using Cellmax/Miniperme

Bioreactors (Unisyn Technologies, Hopkinton, MA, USA). Supernatants were then harvested, concentrated using Amicon centrifugal units (100 000 MWCO, Millipore, Cork, Ireland) and mAbs were purified using Protein A sepharose chromatography (Pharmacia, Uppsala, Sweden). The Ig isotypes of mAbs were determined by using an Ig Isotyping Kit (Amersham, Buckinghamshire, UK).

Cell culture and transfections. HEK293T cells were maintained in Dulbecco's Modified Eagle Medium (DMEM) supplemented with 10% foetal bovine serum (FBS) and cultured according to the standard mammalian tissue culture protocols and sterile technique. Cells cultured on 10-cm dishes were transiently transfected using Fugene 6 reagent (Roche) according to the manufacturer's instructions.

Immunoprecipitation and western blotting. Cells were lysed in 20 mM Tris-pH 7.4, 135 mM NaCl, 1.5 mM MgCl₂, 1 mM ethylene glycol tetraacetic acid, 10% glycerol and 1% Triton X-100 supplemented with Complete protease inhibitor cocktail tablets (Roche). Protein concentration was determined using a BCA assay (Thermo Fisher Scientific, Houston, TX, USA). Cell lysates were incubated with pre-washed protein G-sepharose beads for 1 h at 4 °C with gentle agitation. The pre-cleared lysates were incubated with protein G-sepharose beads and antibodies against HA (3F10, Roche) or Bcl-G (2E11). Protein complexes were detected on western blots with rat monoclonal antibodies to Bcl-G or HA (3F10, Roche) and mouse monoclonal antibodies to HSP70 (used as a loading control). Goat anti-mouse or anti-rat IgG antibodies conjugated to HRP (Southern Biotechnology, Birmingham, AL, USA) were used as secondary reagents and chemiluminescence (ECL, GE Healthcare, Buckinghamshire, UK) was used for detection of protein bands.

Tissue immunohistochemistry. Mouse tissues were fixed in 10% buffered formalin and embedded in paraffin blocks. For immunohistochemistry, sections were dewaxed in xylene, rehydrated in successive ethanol baths and microwaved in 10 mM citric acid buffer pH 6. Aldehydes were quenched with 0.2-M glycine and endogenous peroxidases blocked by incubation with 3% H₂O₂ in methanol. Nonspecific binding of antibodies was blocked by incubation with 5% normal goat serum, 1% BSA and 0.3% Triton X-100. Sections were incubated with anti-Bcl-G mAb clone 2E11 (5 µg/ml) overnight at 4 °C. After washing with PBS containing 0.03% Triton X-100, biotinylated goat anti-rat-IgG2a antibodies (Vector Laboratories, Burlingame, CA, USA) were applied. This was followed by staining with the ABC Vectastain Elite reagent (Vector Laboratories) and finally detection with DAB reagent (Vector Laboratories) and counterstaining with hematoxylin.

Immunofluorescence. 293T cells were grown on cover slips and transiently transfected with mammalian expression vectors using Fugene 6 (Roche). Forty-eight hours post transfection, cells were incubated with Mitotracker Red (Molecular Probes) diluted to a final concentration of 100 nM for 30 min at 37 °C to stain the mitochondria before fixing in 4% paraformaldehyde and permeabilisation with 0.2% TX-100. Subcellular localisation of Bcl-G was detected by staining with mAb 2E11 for 1 h, followed by incubation with Alexa488-labelled goat anti-rat Ig secondary antibodies (Molecular Probes). Nuclei were then stained using DAPI, followed by cover slip mounting using fluorescent mounting media (Dako, Glostrup, Denmark). Microscopy was performed on an LSM5 laser-scanning microscope (Carl Zeiss, Oberkochen, Germany), visualising the mitochondria (as red), Bcl-G (as green) and nuclei (as blue).

Intracellular staining for flow cytometric analysis. Transiently transfected 293T cells (5×10^5) were fixed in 1% paraformaldehyde, washed and permeabilised with 0.3% saponin (Sigma Chemicals, Rowville, Victoria, Australia). The cells were then incubated with various dilutions of hybridoma supernatants or purified antibodies for 1 h on ice. Bound antibodies were detected with FITC-conjugated goat anti-rat IgG secondary antibodies (Southern Biotechnology) and cells analysed in a FACScan (Becton Dickinson, North Ryde, NSW, Australia). Staining with an antibody against the HA epitope tag (3F10, Roche) was used as a positive control. For intracellular staining of DCs, Bcl-G mAbs were biotinylated according to the manufacturer's instructions (Molecular Probes) and staining detected with phycoerythrin (PE)-streptavidin (BD Pharmingen, San Diego, CA, USA).

DC enrichment. DCs were isolated from the spleens of mice as described.¹⁶ Briefly, mouse spleens were digested in modified RPMI-1640 medium, 2%

FBS (FCS)-containing collagenase (1 mg/ml, Worthington Biochemicals, Lakewood, NJ, USA) and DNase (0.02 mg/ml, Roche) for 20 min at RT. EDTA (7 mM) was added for 5 min to disrupt DC-T cell rosettes and inhibit collagenase activity. Cell suspensions were passed through sieves and cells recovered by centrifugation. Cells were then resuspended in Nycodenz-EDTA (Nycomed, Oslo, Norway) at 1.077 g/cm³ (5 ml per four mice) and layered onto an equal volume of fresh Nycodenz-EDTA of the same density, followed by an overlay of EDTA-FCS. Density separation was performed at 1700 r.p.m. for 10 min. Cells within the light density fraction were collected into a new tube and washed with a divalent metal-free buffered balanced salt solution containing EDTA (BSS-EDTA), followed by antibody staining for FACS analysis.

Conflict of Interest

The authors declare no conflict of interest.

Acknowledgements. We thank M Robati for technical assistance, LA O'Reilly for sharing reagents and expertise, G Siciliano, J Coughlin, E Sutherland and S O'Connor for mouse care, B Helbert and C Young for mouse genotyping, K Wycherley for mAb production, E Tsui, S Mihajlovic and their team for histological preparations. This work was supported by the Australian NHMRC (programme grant 461221, Independent Research Institutes Infrastructure Support Scheme grant 361646 and Career Development Award), the Leukaemia and Lymphoma Society (Specialized Centre of Research Grant 7015), and infrastructure support from the NHMRC (IRISS) and the Victorian State Government (OIS). M Giam was funded by the University of Melbourne under the Endeavour IPRS scholarship programme. JD Mintern is the recipient of an NHMRC Career Development Award.

1. Strasser A, Cory S, Adams JM. Deciphering the rules of programmed cell death to improve therapy of cancer and other diseases. *EMBO J* 2011; **30**: 3667–3683.
2. Youle RJ, Strasser A. The BCL-2 protein family: opposing activities that mediate cell death. *Nat Rev Mol Cell Biol* 2008; **9**: 47–59.
3. Lomonosova E, Chinnadurai G. BH3-only proteins in apoptosis and beyond: an overview. *Oncogene* 2008; **27**(Suppl 1): S2–19.
4. Guo B, Godzik A, Reed JC. Bcl-G, a novel pro-apoptotic member of the Bcl-2 family. *J Biol Chem* 2001; **276**: 2780–2785.
5. Miled C, Pontoglio M, Garbay S, Yaniv M, Weitzman JB. A genomic map of p53 binding sites identifies novel p53 targets involved in an apoptotic network. *Cancer Res* 2005; **65**: 5096–5104.
6. Montpetit A, Larose J, Boily G, Langlois S, Trudel N, Sinnett D. Mutational and expression analysis of the chromosome 12p candidate tumor suppressor genes in pre-B acute lymphoblastic leukemia. *Leukemia* 2004; **18**: 1499–1504.
7. Kibel AS, Huagen J, Guo C, Isaacs WB, Yan Y, Pienta KJ *et al*. Expression mapping at 12p12-13 in advanced prostate carcinoma. *Int J Cancer* 2004; **109**: 668–672.
8. Pickard MR, Green AR, Ellis IO, Caldas C, Hedge VL, Mourtada-Maarabouni M *et al*. Dysregulated expression of Fau and MELK is associated with poor prognosis in breast cancer. *Breast Cancer Res* 2009; **11**: R60.
9. Pickard MR, Edwards SE, Cooper CS, Williams GT. Apoptosis regulators Fau and Bcl-G are down-regulated in prostate cancer. *Prostate* 2010; **70**: 1513–1523.
10. Lin ML, Park JH, Nishidate T, Nakamura Y, Katagiri T. Involvement of maternal embryonic leucine zipper kinase (MELK) in mammary carcinogenesis through interaction with Bcl-G, a pro-apoptotic member of the Bcl-2 family. *Breast Cancer Res* 2007; **9**: R17.
11. Nakamura M, Tanigawa Y. Characterization of ubiquitin-like polypeptide acceptor protein, a novel pro-apoptotic member of the Bcl2 family. *Eur J Biochem* 2003; **270**: 4052–4058.
12. Nakamura M, Yamaguchi S. The ubiquitin-like protein MNSFbeta regulates ERK-MAPK cascade. *J Biol Chem* 2006; **281**: 16861–16869.
13. O'Reilly LA, Cullen L, Moriishi K, O'Connor L, Huang DCS, Strasser A. Rapid hybridoma screening method for the identification of monoclonal antibodies to low abundance cytoplasmic proteins. *BioTechniques* 1998; **25**: 824–830.
14. Herzog EL, Brody AR, Colby TV, Mason R, Williams MC. Knowns and unknowns of the alveolus. *Proc Am Thorac Soc* 2008; **5**: 778–782.
15. Wilson IA, Niman HL, Houghten RA, Cherenon AR, Connolly ML, Lerner RA. The structure of an antigenic determinant in a protein. *Cell* 1984; **37**: 767–778.
16. Vreemec D, Pooley J, Hochrein H, Wu L, Shortman K. CD4 and CD8 expression by dendritic cell subtypes in mouse thymus and spleen. *J Immunol* 2000; **164**: 2978–2986.



Cell Death and Disease is an open-access journal published by Nature Publishing Group. This work is licensed under the Creative Commons Attribution-NonCommercial-No Derivative Works 3.0 Unported License. To view a copy of this license, visit <http://creativecommons.org/licenses/by-nc-nd/3.0/>